



The Open Mechanical Engineering Journal

Content list available at: www.benthamopen.com/TOMEJ/

DOI: 10.2174/1874155X0161001032;



A Theoretical Analysis on Bone Drilling Temperature Field of Superhard Drill

Yali Hou, Changhe Li*, Hongliang Ma, Yanbin Zhang, Min Yang and Xiaowei Zhang

School of Mechanical Engineering, Qingdao Technological University, 266520 Qingdao, China

Received: October 9, 2015

Revised: December 7, 2015

Accepted: January 21, 2016

Abstract: To overcome strong drilling force and over high temperature during orthopedic surgery, the four medical drills with different geometrical shapes by using superhard materials were designed. The bone drilling temperature field of superhard drill was theoretical analyzed. Results showed that brazed step drill has the most ideal drilling temperature. It controls the maximum bone temperature below 47°C even under dry drilling. The maximum bone temperature of brazed twist drill is a little higher than 47°C. With appropriate cooling method, brazed twist drill also could provide ideal effect. On the contrary, drilling temperatures of common twist drill, brazed abrasive drill and brazed PCBN superhard drill increase successively. All of them are far higher than the critical temperature of osteonecrosis. The maximum temperatures of brazed step drill, brazed twist drill, common twist drill, brazed abrasive drill and brazed PCBN superhard drill under steady state at about 45.9°C, 61.5°C, 70.5°C, 101.2°C and 113.2°C, respectively. Brazed step drill shows the lowest drilling temperature, followed by brazed twist drill, standard twist drill, brazed abrasive drill and brazed PCBN superhard drill successively.

Keywords: Bone drilling, Critical temperature, Osteonecrosis, Superhard drill, Temperature field.

1. INTRODUCTION

Bone fracture exists throughout the human history. People's understanding and therapy of bone fracture are developing continuously. There's written record in western countries that mixture of earth and gum as well as mixture of egg white and flour was used for fracture fixation. The popular fracture treatment with gypsum and bandage was invented by European. This treatment is known as today's closed reduction and external fixation [1]. Closed reduction and external fixation is to restore broken bones firstly by tact or continuous traction, followed by external fixation with gypsum and bandage. The external fixation must cover adjacent joints to the bone fracture. Such treatment avoids open reduction and thereby protects fracture hematoma and periosteum, beneficial for fracture healing. However, although it heals fracture quicker than open reduction, its long-time external fixation will cause ankylosis and muscular atrophy which take a long time for physiotherapy and exercise to recover functions. Elders are even difficult to recover completely.

Nowadays, serious bone fracture prefers open reduction and internal fixation to external fixation. Open reduction and internal fixation cuts soft tissue to expose bone fracture directly or only cut the position for internal fixation rather than the bone fracture. After reduction of fracture, metal bone fracture plate, fastening screw, intramedullary nail, steel wire or biological synthetic materials which are highly compatible with body are used as internal fixation of the fracture. Although internal fixation ensures high-precision reduction of fracture and shortens postoperative recovery significantly, it has many potential adverse factors, because it attaches high attention on reduction and fixation during surgery and adopts much external interventions, but neglects living tissue of bones. It destroys fracture hematoma, hurts periosteum and surrounding soft tissue, as well as weakens or even cuts off local blood supply, thus resulting in delayed

* Address correspondence to this author at the School of Mechanical Engineering, Qingdao Technological University, 266520 Qingdao, China; Tel:+86-532-68052760; Fax: +86-532-85071286; E-mail: sy_lichanghe@163.com

fracture healing [2]. Though modern metal internal fixations have good biocompatibility with human bodies, this is not absolutely right. Additionally, internal factors of design or materials could affect physical properties of internal fixation materials, making them bent or broken. This will cause fracture displacement and malunion. Open reduction increases possibility of infection and operative complications. Once infection occurred, the internal fixation materials become foreign matters that are difficult to be compatible with human bodies. For tightening fixation, internal fixation materials are often fixed tightly on backbones or in marrow cavity. Since bone reacts to local pressure by bone absorption, internal fixation materials will be loosed and couldn't fix the fracture after a certain time. During orthopedic surgery, it is necessary to drill holes on fracture for screws to fix bone fracture plate and intramedullary nails. However, drilling is easy to generate over high temperature at the hole, which will kill bone cells. This will prolong recovery of patients or even operation failure.

Due to the obvious superiority to existing fracture treatments, open reduction is applied more and more in clinical operation. However, it is not perfect and will also cause new problems. Accurate fracture reduction of bone surgery is attributed to internal fixation of metal bone fracture plate and intramedullary nails with screws. Such extruding fixation has high requirements on stability and safety of fixing threads [3]. As a result, failure of fixing threads will cause final failure of the operation. Investigations reported 2.1%~7.1% [4, 5] failure operation caused by failure of fixing threads. One important cause to failure of fixing threads is that over high bone drilling temperature kills bone cells and brings irreversible changes to bone structure and physical properties, thus increasing bone absorption surrounding screws that are fixed inside bones. Annular osteonecrosis caused by high temperature has been observed under X-ray. It also discovered thermal necrosis of bone cells when living bone cells stay under 47°C for 1min [6].

Orthopedic drill is one of important instruments in orthopedic surgery. It is mainly used for drilling blind hole or through-hole at drumhead, skull, dentale and common human bones [7]. In practical orthopedic bone hole drilling, the surgeon must apply an appropriate axial force to ensure the hole drilling stable and smooth. However, bone drilling is different from metal cutting. Bone, a kind of unique multi-org composite, is composed of organics and inorganics. It will suffer very complicated deformation and forces during drilling. Moreover, considering severe conditions in practical surgery, orthopedic drill shall be designed and manufactured with sharp cutting edge, adequate stiffness and toughness, as well as high processing precision. In particular, it shall be excellent heat dissipation to control drilling temperature below 47°C. This not only could improve drilling quality and fixation effect of implantation materials, but also shortens recovery time of patient significantly.

Abundant exploratory researches on bone drilling temperature during orthopedic surgery have been reported. They mainly involve the following three aspects. Some focused on influence law of drilling parameters (*e.g.* speed of mainshaft, load and axial pressure) on bone drilling temperature. Subsequently, they chose optimized drilling parameters to control drilling temperature reasonably. Since it is difficult to use uniform variables in experiments, including experimental facility, temperature measuring equipment and bone materials, no agreed influence law of drilling parameters on bone drilling temperature has been reached yet. Some scholars tried to design new orthopedic drills to overcome strong drilling force, difficult drillings removal and over high temperature of traditional medical drills. Although some new orthopedic drills lower bone drilling temperature to a certain extent, they still used material cutting mechanism of continuous cutting edge and failed to control the drilling temperature strictly within the critical value of human bodies (<47°C). They didn't solve the problem fundamentally. Some other scholars advocated to rinsing the bone with normal saline to lower bone drilling temperature. Although it is widely used in practical surgery, it is difficult for cooling liquid to reach to the drilling zone, restricting the cooling effect of normal saline greatly.

Many scholars studied critical temperature of osteonecrosis during orthopedic surgery. Augustin and Davila *et al.* [8] made a bone drilling experiment. They used thigh bone of 8~10-month-old pig with 4~5mm thick compact bone substance as testing material. Thermocouple with a measuring range of -40~1200°C was used as the temperature measurer. The response time was less than 0.1s. ALG-100 drill which has several optional rotate speeds and feed rates was used. All applied testing equipments were checked and calibrated before the experiment. Firstly, a small hole was drilled and the thermocouple was bonded at 3mm depth of the hole. Every hole was located by a guiding device. The distance between drilling hole and the hole with thermocouple was kept 0.5mm. Three drills with different diameters (2.5mm, 3.2mm and 4.5mm) were used. The experiment was implemented in laboratory under 84mm/min feed rate and 188r/min, 462r/min, 1140r/min and 1820r/min speed of mainshaft. Temperature was kept 26°C throughout the whole experiment. According to the test data, bone drilling temperature increases with the acceleration of mainshaft.

Rafel [9] carried out an experimental study on high rotate speed and bone drilling temperature, but got conflicting results. He used a series of medical drills with different shapes to drill holes on upper jaw bone of human bodies

without external pouring cooling. The final results showed that from 10,000r/min~350,000r/min, the maximum temperature is at 10,000r/min. This reflects that bone drilling temperature decreases with the acceleration of mainshaft.

To analyze effect of drilling speed on bone drilling temperature, Yang and Wang *et al.* [10] implemented drilling experiment on fresh pig tibia with different medical drills. The final experimental result reveals a proportional relationship between drilling speed and drilling temperature.

In the bone drilling experiment, Udiljak and Ciglar *et al.* [11] explored the influence law of cutting feed on drilling temperature by using a 4.5mm drill. The cutting feeds were 0.02mm, 0.06mm and 0.1mm, and the cutting speeds were set 6m/min, 8m/min, 10m/min, 12m/min, 14m/min and 16m/min. Final result showed that bone drilling temperature decreases with the increase of cutting feed.

Larry and Matthews *et al.* [12] made a series of experiments on human femoral shaft. They paid attentions to effect of axial force on bone drilling temperature. They used four 0.25mm NiCr-NiAl shielded thermocouples to measure drilling temperature. Wire of thermocouple was connected with four amplifiers and its signal was recorded by the galvanometer for recording ultraviolet ray. The response time for thermocouple reaches 100°C was smaller than 6ms. To measure drilling axial force, the sample support was suspended on a steel cantilever with an electronic gauge. Output signals were recorded by the galvanometer for recording ultraviolet ray after being amplified. In the experiment, location of thermocouple and drilling holes were controlled by guide pad. The distances from thermocouple to drilling holes were 0.5mm, 1.0mm, 2.0mm and 3.0mm, respectively. Before the experiment, Ringer's solution flows cyclically in the marrow cavity, which is to maintain sample temperature at about 37°C. The speed of mainshaft was 2900r/min and the drill diameter was 3.2mm. Experimental data demonstrated that bone drilling temperature decreases with the increase of axial force.

Vaughn and Peyton [13] drilled holes on dentine under axial load range of 1~2 pounds (1 pound ≈0.4536kg). The final test data showed that with the increase of axial force, bone drilling temperature rises. This disagrees with the results of Matthews and Hirsch.

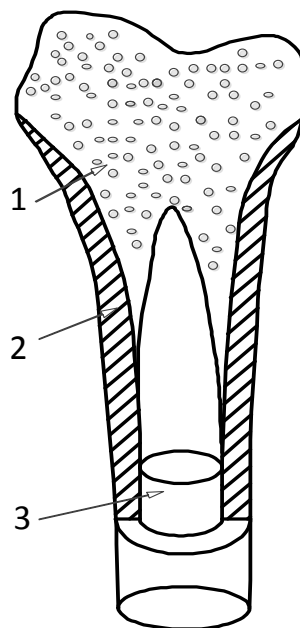
Sorenson [14] drilled dentine without pouring cooling liquid. He concluded that within 0.3~0.5N of axial force, drilling temperature shows an inverse "V-shaped" variation law.

Although many scholars [15 - 48] have carried out a lot experiments, their experimental results disagree with each other and some are even conflict. This may be caused by variation reasons. Firstly, different testing materials like human bones, ox bones and pig bones have different mechanical and thermal properties. Secondly, these experiments were implemented under different conditions. Some applied normal saline for pouring cooling, while some employed no cooling measures. Thirdly, these experiments used different drilling equipments and measuring devices. No uniform standard of processing precision and measurement accuracy was available. Fourthly, these scholars lacked corresponding mathematical models and simulations to support their experimental results.

2. PROCESSING CHARACTERISTICS OF BONE MATERIALS

As a special connective tissue with good toughness and stiffness, human bones are characteristic of anisotropism. Bone contains porous calcification materials. There are abundant bone salts in intercellular substances. Bone salts are mainly composed of 84% calcium phosphate, 10% calcium carbonate, 2% calcium citrate and 2% disodium hydrogen phosphate. They distribute in organic matters of bones as amorphous calcium phosphate and hydroxyapatite crystals. Organic matters of bones mainly consist of collagen fiber, accounting for 95% of organic intercellular substances of bone tissue [15].

Macrostructure of adult thighbone is shown in Fig. (1). Two distinct structural tissues could be seen by separating the thighbone vertically. The hard and compact bone tissue on surface is called as compact bone. Many irregular rod-shaped or lamellar bone tissues at center and two ends are called as bone trabecula. They interconnect into sponge and are also called as cancellous bone. Cancellous bone cavities connect with each other and are filled with hemopoietic tissues and blood vessels, known as bone marrow. Compact bone is a kind of compact material with about a specific gravity of 2. Its external surface is covered by a layer of periosteum and its internal surface is covered by endosteum. Cancellous bone is formed by irregular parallel arrangements of several layers of bone lamella. They interconnect into a grid structure with uneven mesh sizes. It is visible that meshes are filled with bone marrow, blood vessels and nervous systems, which provide nutrition and oxygen for growth and repair of periosteum and endosteum. Therefore, meshes of cancellous bone are actually marrow cavities.



1—cancellous bone 2—compact bone 3—bone marrow

Fig. (1). Macrostructure of adult thighbone.

Human bones are composed of organics and inorganics. Proportions of organics and inorganics in human bones vary at different growth stages. Hence, bones of different ages have different physical properties. Scholars have been interested in studying mechanical properties of healthy adult human bones and achieved satisfying results. Mean mechanical, thermal and physical properties of adult human bones and pig bones are listed in Table 1 [16, 17].

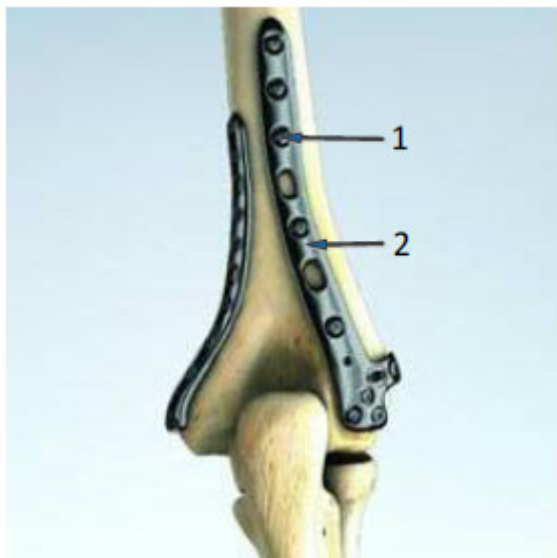
Table 1. The properties of material.

Materials	Density (kg/m ³)	Shearing strength(Mpa)	Specific heat (J/Kg•K)	Coefficient of heat conduction(W/m•k)
human bone	2200	82	1150	2.2
pig bone	2010	75	1330	1.7

Although bone materials have different components and metals, bone deformation during cutting can be divided into three stages, namely, elastic deformation stage, plastic deformation stage and fracture stage. Influenced by load gradually, bone firstly show elastic deformation which shifts to plastic deformation after stress reached the yield stress. As stress continues to increase to the limit, bone materials get damaged and finally broken [18].

In practical clinical orthopedic surgery, different positions of bone fracture may adopt different treatments, but the basic steps are similar. During surgery preparation, patients have to get X-ray to determine location and degree of bone fracture. Next, local anesthesia or general anesthesia will be implemented. During the surgery, the surgeon will choose an appropriate position to cut the fracture position and then uses a periosteal detacher to peel off the periosteum for drilling holes. Subsequently, the surgeon drills holes with an electronic drill and controls the drilling by his / her feeding force. This brings great risks to drilling. To prevent drilling out, researchers are committed to developing an auto-stop medical electric drill. After finished the drilling, tightening screws and bone fracture plate will be used to fix the bone fracture Fig. (2), followed by wound closure and postoperative recovery [18, 19].

Bone drilling quality determines postoperative recovery of patients. In the past, surgery usually uses electric hand drill and one-time continuous drilling way which requires the surgeon having rich clinical experiences. Moreover, it is difficult to locate the holes accurately during the drilling process. Currently, surgeons often employ twice drilling way: pre-drilling and secondary reaming. The pre-drilling improves location accuracy of holes greatly and limits temperature rise of bone tissue to a certain extent. Meanwhile, the secondary reaming provides an accurate location reference point, preventing slipping and malposition during bone drilling effectively.

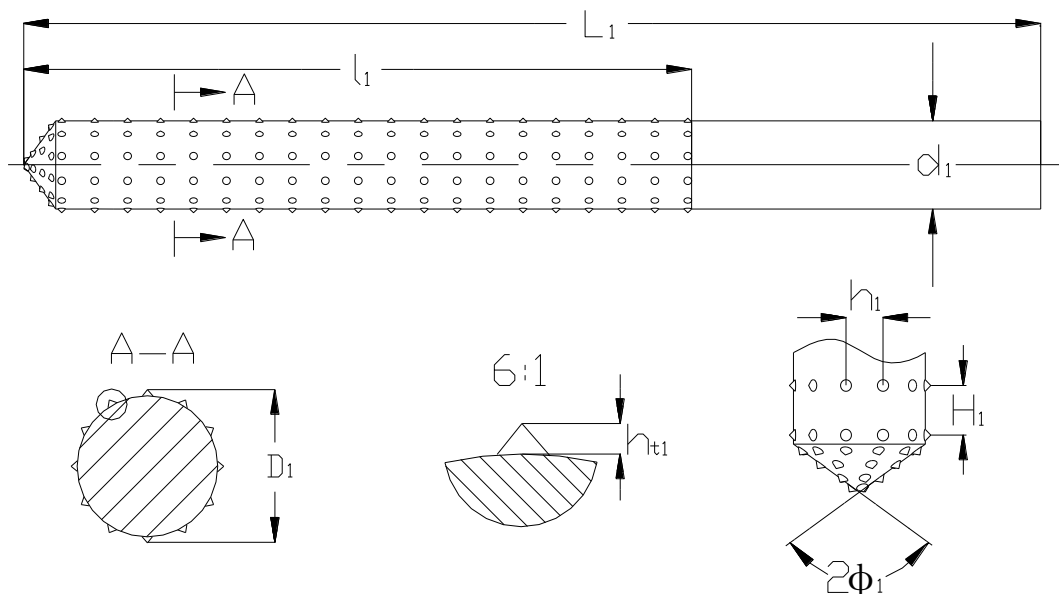


1—tightening screws 2—bone fracture plate

Fig. (2). Schematic diagram of fractures fixed.

3. DESIGN OF SUPERHARD ORTHOPEDIC DRILL

To overcome strong drilling force and over high temperature during orthopedic surgery, the author [20 - 23] attempted to design three medical drills with different geometrical shapes by using brazed diamond technology with controllable abrasive particle arrangement: brazed abrasive drill, brazed twist drill and brazed step drill (Figs. 3-5).

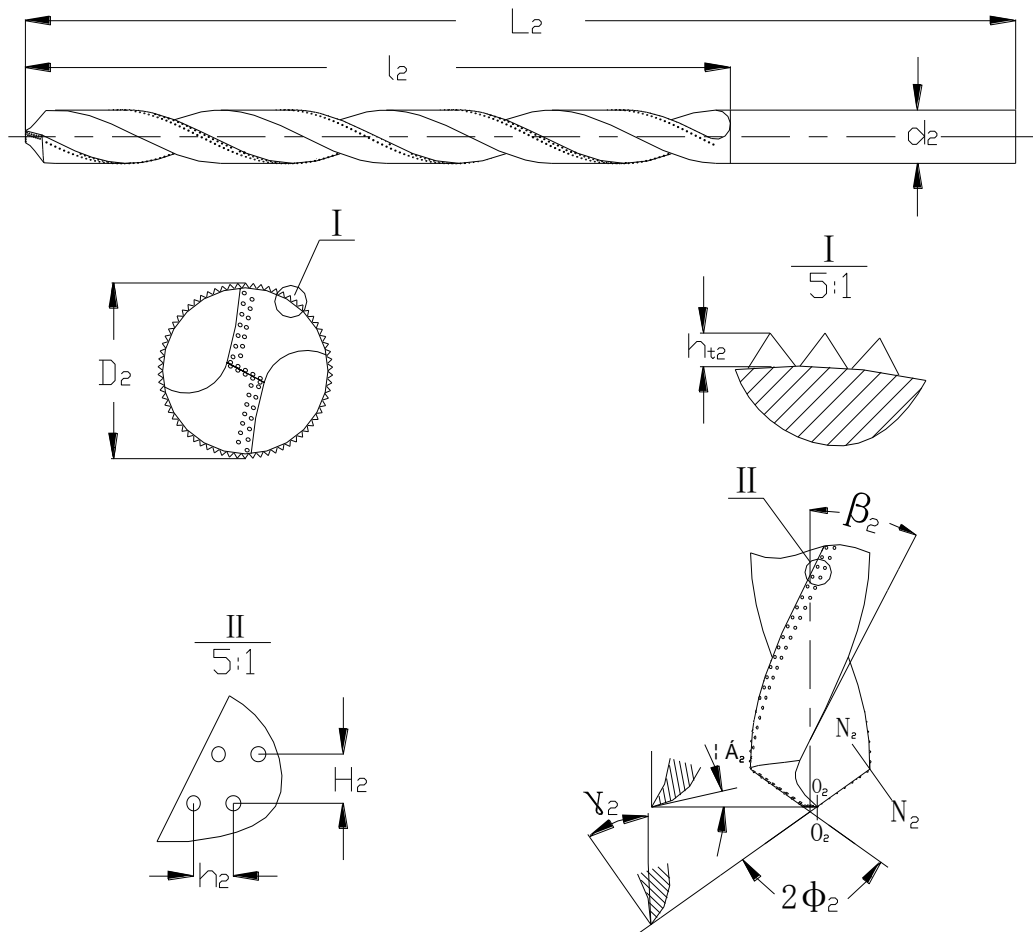


L_1 — total length of brazed abrasive drill; l_1 — length of the working part of brazed abrasive drill; $2\Phi_1$ — apex angle of the cone; d_1 — substrate diameter of brazed abrasive drill; h_{t1} —protrusion height of single abrasive particle of brazed abrasive drill; H_1 — line spacing of diamond abrasive particles of brazed abrasive drill; h_1 — space between diamond rows of brazed abrasive drill; D_1 — mean diameter of the brazed abrasive drill

Fig. (3). Geometric structure of brazed abrasive drill.

The substrate of brazed abrasive drill is a piece of cylinder bar with cone ends. Brazed diamond technology with

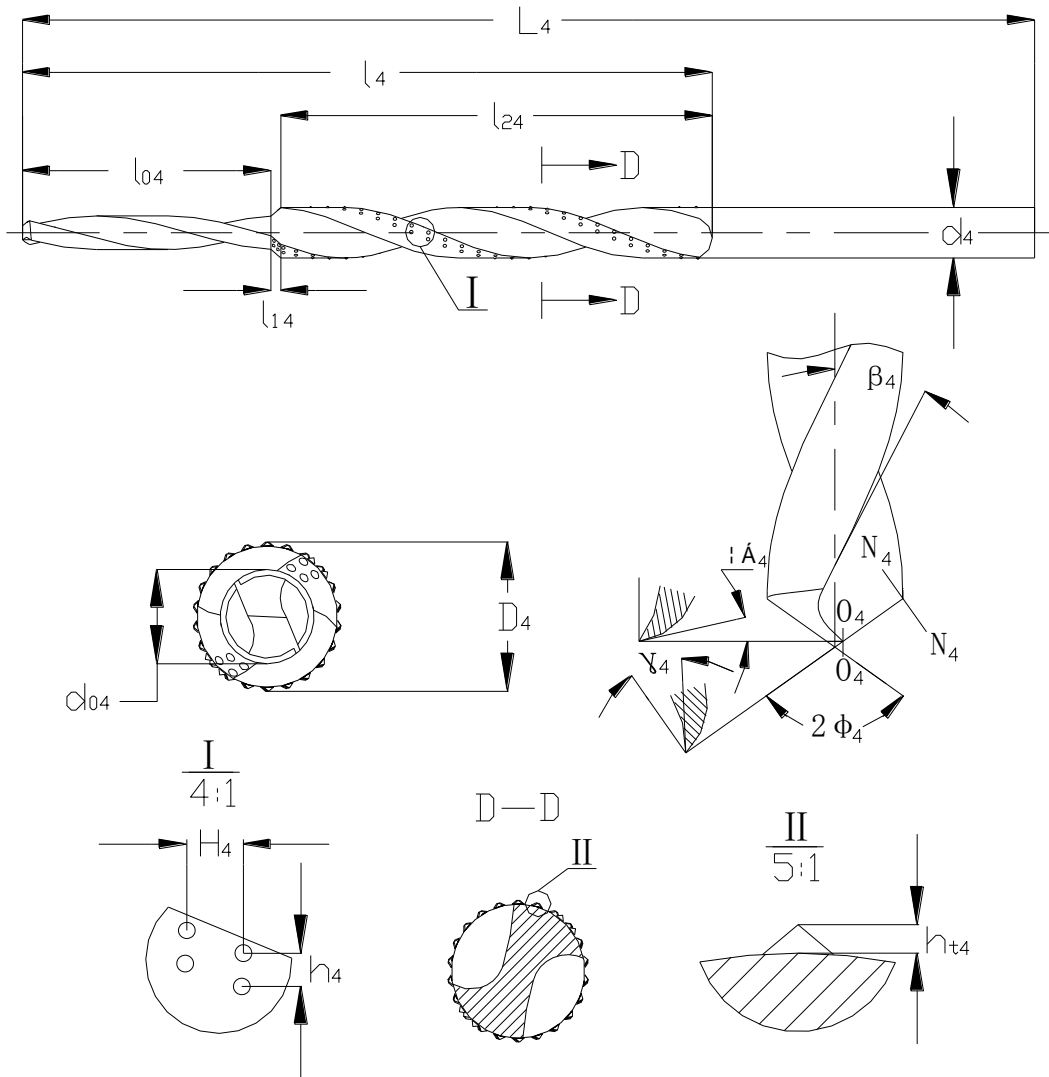
controllable abrasive particle arrangement is implemented on the substrate surface. It not only ensures enveloping and embedding capabilities of diamond, but also controls protrusion height. Distance between abrasive particles could be adjusted as needed. The brazed diamond technology with controllable abrasive particle arrangement could maintain as high as 70%~80% protrusion heights of diamond abrasive particles, but also control arrangement of abrasive particles. This gives the drill adequate spaces for drillings. The drill could remove drillings timely, carry away generated heats and lowers temperature.



L_2 — total length of brazed twist drill; d_2 — substrate diameter of brazed twist drill; l_2 —length of the working part of brazed twist drill; $2\Phi_2$ — apex angle of brazed twist drill; β_2 — helix angle of brazed twist drill; γ_2 — front angle of brazed twist drill; α_2 — back angle of brazed twist drill; h_{t2} —protrusion height of single abrasive particle of brazed twist drill; D_2 — mean diameter of the brazed twist drill; H_2 —line spacing of diamond abrasive particles of brazed twist drill; h_2 —space between diamond rows of brazed twist drill

Fig. (4). Geometric structure of brazed twist drill.

The substrate of brazed twist drill is common standard twist drill. Brazed diamond technology with controllable abrasive particle arrangement is implemented at the main cutting edge and minor cutting edge. It uses aligned and regular diamond abrasive particles instead of traditional twist cutting edge and an intermittent cutting rather than traditional continuous cutting. Spacing between diamond abrasive particles also is adjustable according to practical needs.



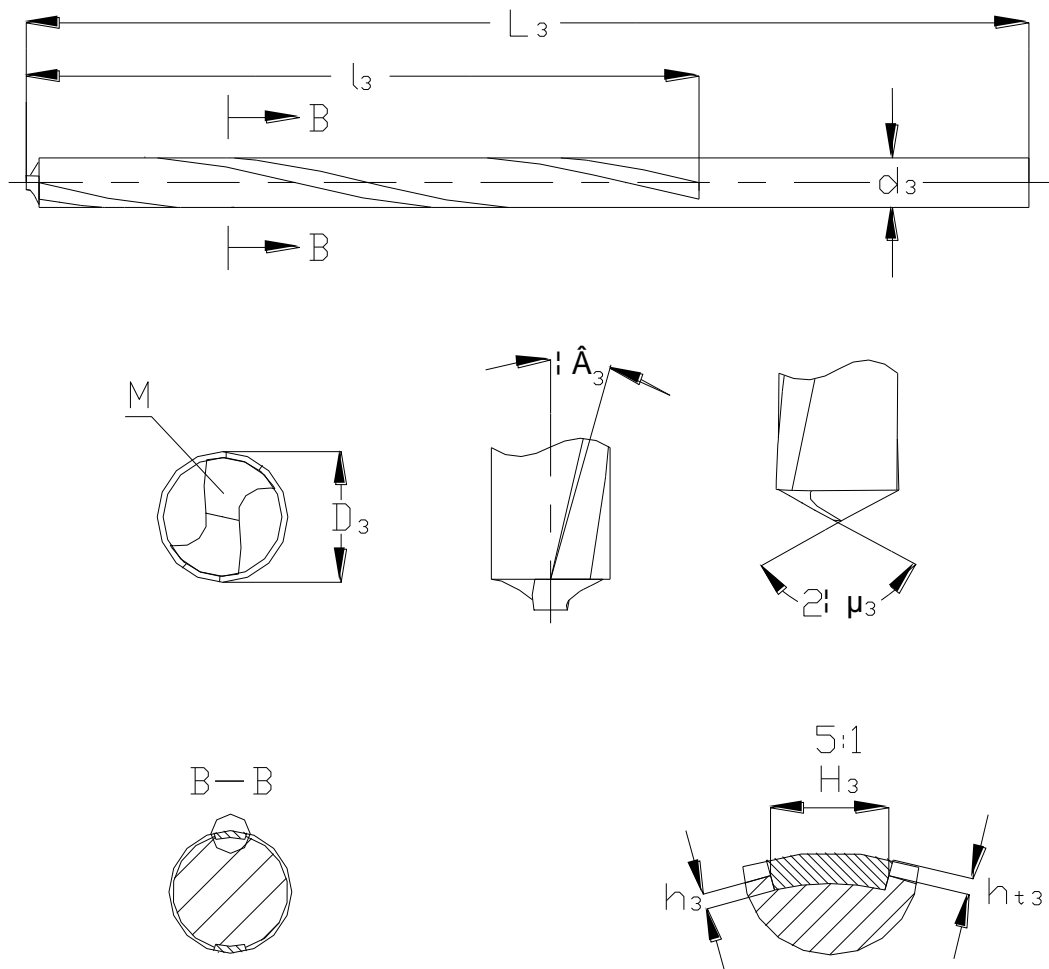
L_4 —total length of brazed step drill; l_4 — length of the working part of brazed step drill; d_4 —substrate diameter of brazed step drill; β_4 —helix angle of brazed step drill; l_{04} — drilling part; d_{04} — diameter of drilling part; $2\Phi_4$ — apex angle of brazed step drill; γ_4 — front angle of brazed step drill (N_4 — N_4 profile); α_4 — back angle of brazed step drill (O_4 — O_4 profile); l_{14} — transition part; l_{24} — reaming part; H_4 —line spacing of diamond abrasive particles of brazed step drill; h_4 —space between diamond rows of brazed step drill; h_{t4} —protrusion height of single abrasive particle of brazed step drill; D_4 — mean diameter of brazed step drill.

Fig. (5). Geometric structure of Brazed step drill.

Brazed step drill has similar appearance with common step drill. The whole working part can be further divided into three parts: drilling part, transition part and reaming part. The drilling part has a small diameter and could reduce axial force effectively. Brazed diamond technology with controllable abrasive particle arrangement is implemented at the minor cutting edge of transition part and reaming part. It uses aligned and regular diamond abrasive particles rather than cutting edge of traditional twist drill.

Brazed PCBN Superhard drill is shown in Fig. (6). The drill tip is similar with that of common straight shank twist drill. Firstly, a drill tip similar with that of common twist drill is processed at one end of the cylinder substrate. Shape parameters of the drill tip are same with those of standard twist drill tip. Secondly, a spiral groove (width— H_3 ; depth— h_3) is made on the cylinder substrate surface. Width and depth of the spiral groove could be adjusted according to requirement of the drill. Helix angle of the spiral groove (β_3) varies between 18° ~ 30° , which ensures to remove drillings timely, carry away generated heats and lower temperature. Subsequently, the PCBN superhard material is cut

into plates fitting the flank surface of main cutting edge and the spiral groove. Next, the PCBN superhard plates are brazed on the flank surface of main cutting edge and in the spiral groove. The PCBN superhard material improves sharpness of cutting edge greatly and reduces drilling axial force effectively, finally lowering the drilling temperature.



L_3 — total length of brazed PCBN superhard drill; l_3 — length of working part of brazed PCBN superhard drill; H_3 — width of the spiral groove; h_3 — depth of the spiral groove; β_3 — helix angle of the spiral groove; h_{t3} — substrate protrusion height of cutting edge; d_3 — substrate diameter of brazed PCBN superhard drill; D_3 — diameter of brazed PCBN superhard drill

Fig. (6). Geometric structure of Brazed PCBN Superhard drill.

4. SIMULATION STUDY ON BONE DRILLING TEMPERATURE FIELD

Diameter (d), apex angle (2Φ) and helix angle (β) of the standard twist drill used in simulation were 4mm, 120° and 30° , respectively. Abrasive particles of the drill using brazed diamond technology with controllable abrasive particle arrangement were simplified into uniform spherical rigid bodies. To maintain high drilling efficiency and reduce power consumption, it shall choose bigger diamond abrasive particles. Considering its brazing position and conditions, diameter of the spherical abrasive particle (d) was finally determined 0.5mm, far larger than the required minimum size of brazing diamond. It could meet technological requirements completely. Since protrusion height of abrasive particles in brazing technology could reach 70%~80%, the protrusion height of abrasive particles was set 0.35mm. Spacing between diamond abrasive particles (l) and d_{04} were set $2d$ and 2mm, respectively.

Bone samples were a $\Phi 12 \times 6$ mm cylinders. Standard twist drill, brazed abrasive drill, brazed twist drill, brazed step drill, brazed PCBN superhard drill and bone sample models are presented in Fig. (7a-f).

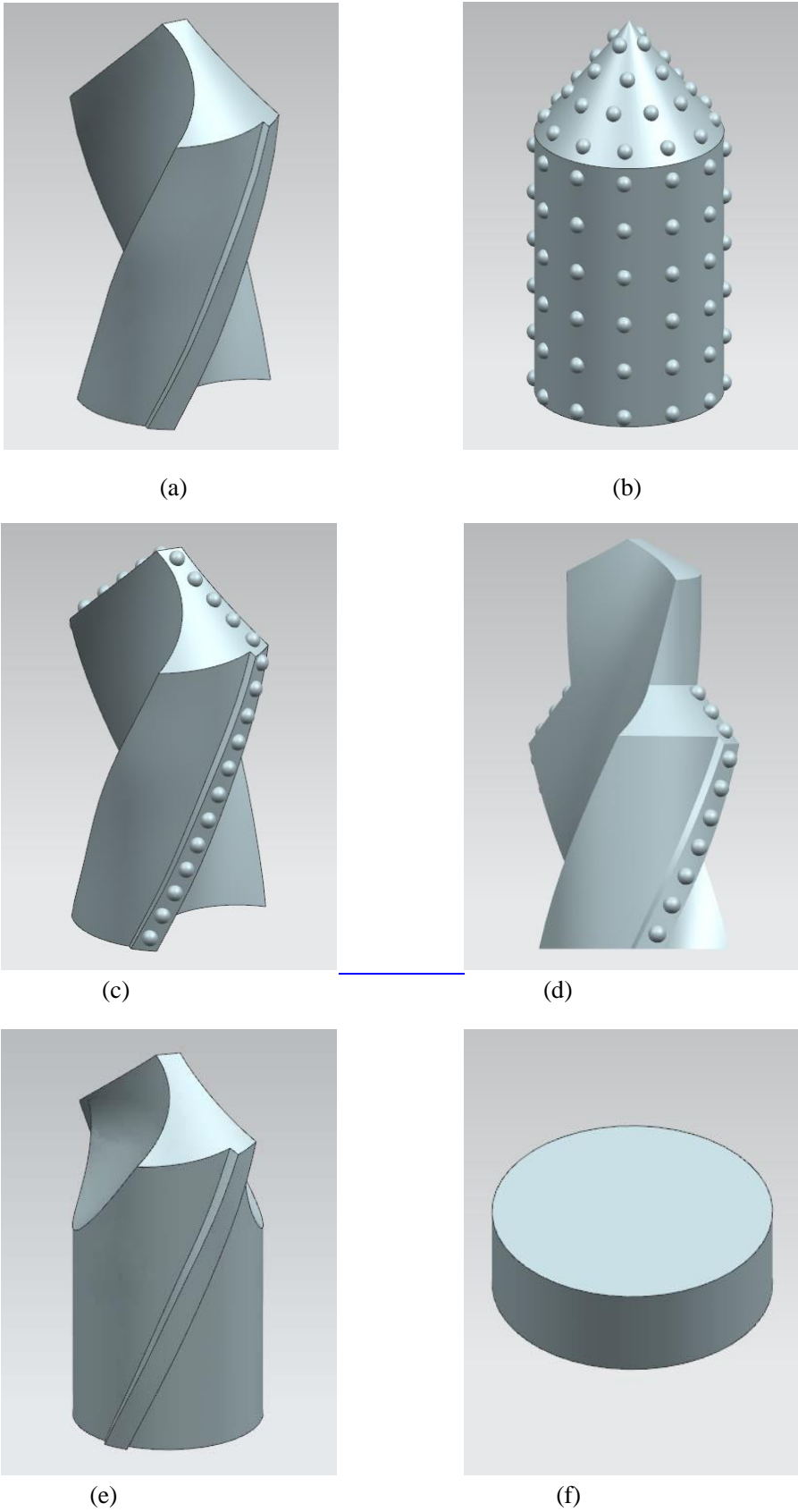


Fig. (7). The model of different drills and bone specimen.

4.1. Material Parameters and Processing Parameters

Substrate of common twist drill and brazed abrasive drill is made of YG8. Main performance parameters of bone sample, diamond abrasive particle, PCBN superhard material and substrate material are listed in Table 2.

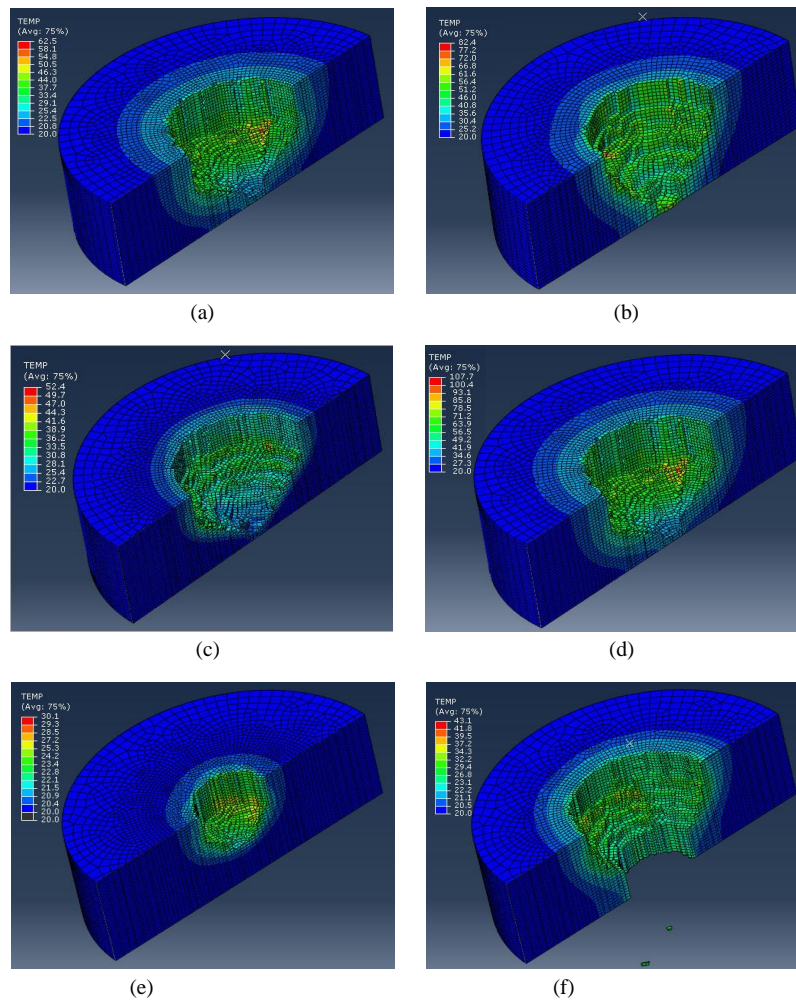
Processing parameters used in simulation are: drill speed $n=1000\text{rpm}$ and feed speed $v_f=0.5\text{mm/s}$.

Table 2. Material properties.

itemsMaterials	density (kg/m^3)	elastic modulus (GPa)	Poisson ratio	specific heat (J/Kg·K)	Coefficient of thermal conductivity (w/m·k)
bone sample	2200	3.5	0.3	1300	2.0
YG8	14500	600	0.22	220	75.4
diamond abrasive particle	3515	1050	0.07	511	2200
PCBN	3480	750	0.25	506	1300

4.2. Initial and Boundary Conditions

During simulation, external environment and constraints of the model have to be defined according to practical clinical operation conditions. Suppose the initial temperature of cutter and bone sample is equal to room temperature (20°C). Since cutter is significantly harder than bone, cutter almost shows no deformation during drilling. Therefore, the drill was defined as rigid body, while bone sample was defined as the deformable body. The whole drilling was set dry drilling. In other words, it used air as cooling medium. Most drilling heats were transferred to bone sample, bone drillings and drill. Only few were transmitted to the external environment through air circulation. Thermal conductivity of air circulation is $15\text{W}/(\text{m}^2\cdot^\circ\text{C})$.



4.3. Temperature Field Distribution on Bone Samples

Temperature field distribution laws on bone samples for standard twist drill, brazed abrasive drill, brazed twist drill and brazed PCBN superhard drill are shown in Fig. (8a-d). The temperature field distribution nephogram on the bone sample for brazed step drill when the drilling part and reaming part reach their steady states are exhibited in Fig. (8e and f).

Heat generated during drilling mainly has three resources: cutting heat converted from power consumption of bone's elastoplastic deformation, friction heat between bone and rake face of the cutter, as well as friction heat between flank surface of the cutter and processed bone surface. Most of these heats are transferred to bone drillings, drill and bone sample. Only few are dissipated through other media. During drilling, it is the chisel edge of the drill that cuts the workpiece firstly. Later, the main cutting edge participates in cutting and undertakes the main cutting task, while the minor cutting edge is mainly responsible for drilling guidance. As the drilling progresses, the maximum temperature appears at the position close to the chisel edge firstly and then dissipates to outer drill edge along the main cutting edge. When heat yield and heat release reach the equilibrium state, the drilling temperature will tend to be stable accordingly. Evident temperature gradient surrounding the drilled bone hole is observed in Fig. (8a-f). Color of this temperature gradient becomes shallow gradually along the radial direction, indicating the decreasing drilling temperature. The maximum temperatures on bone samples using different drills are shown in Fig. (9 drill I, II, III, IV and V) represent brazed step drill, brazed twist drill, common twist drill, brazed abrasive drill and brazed PCBN superhard drill, respectively.

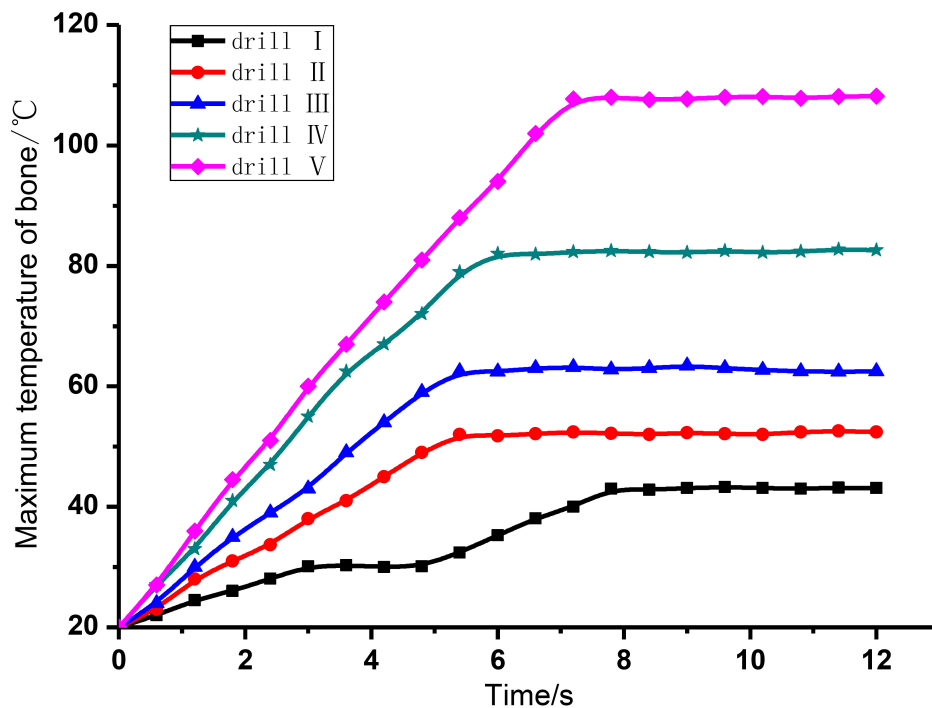


Fig. (9). The maximum temperature on bone samples using different drills.

In Fig. (9), the maximum temperature on bone samples increases as the drilling goes on. Combining (Figs. 8 and 9), the maximum temperatures on bone samples drilled by brazed step drill, brazed twist drill, common twist drill, brazed abrasive drill and brazed PCBN superhard drill under steady state fluctuate toward 43.1°C, 52.4°C, 62.5°C, 82.4°C and 107.7°C, respectively. According to Fig. (9), there are two equilibrium states of the maximum temperature on the bone sample using brazed step drill. These are contributed by the drilling part and reaming part of the brazed step drill. The corresponding maximum temperatures read about 30.1°C and 43.1°C, respectively. Hence, drills with different structures show significantly different drilling temperatures. Brazed step drill shows the lowest drilling temperature and controls it strictly below 47°C, the critical temperature of osteonecrosis. Brazed twist drill achieves the second lowest drilling temperature, a little higher than 47°C. Drilling temperatures of standard twist drill, brazed abrasive drill and brazed PCBN superhard drill increase successively. All of them exceed 47°C greatly.

4.4. Temperature Field Distribution on Drill

Most heats generated during bone drilling are transferred into drill, rising the drill temperature. Temperature field distributions of standard twist drill, brazed abrasive drill, brazed twist drill and brazed PCBN superhard drill at steady state are exhibited in Fig. (10a-d). Temperature field distributions of brazed step drill when its drilling part and reaming part reach steady state are shown in Fig. (10e and f).

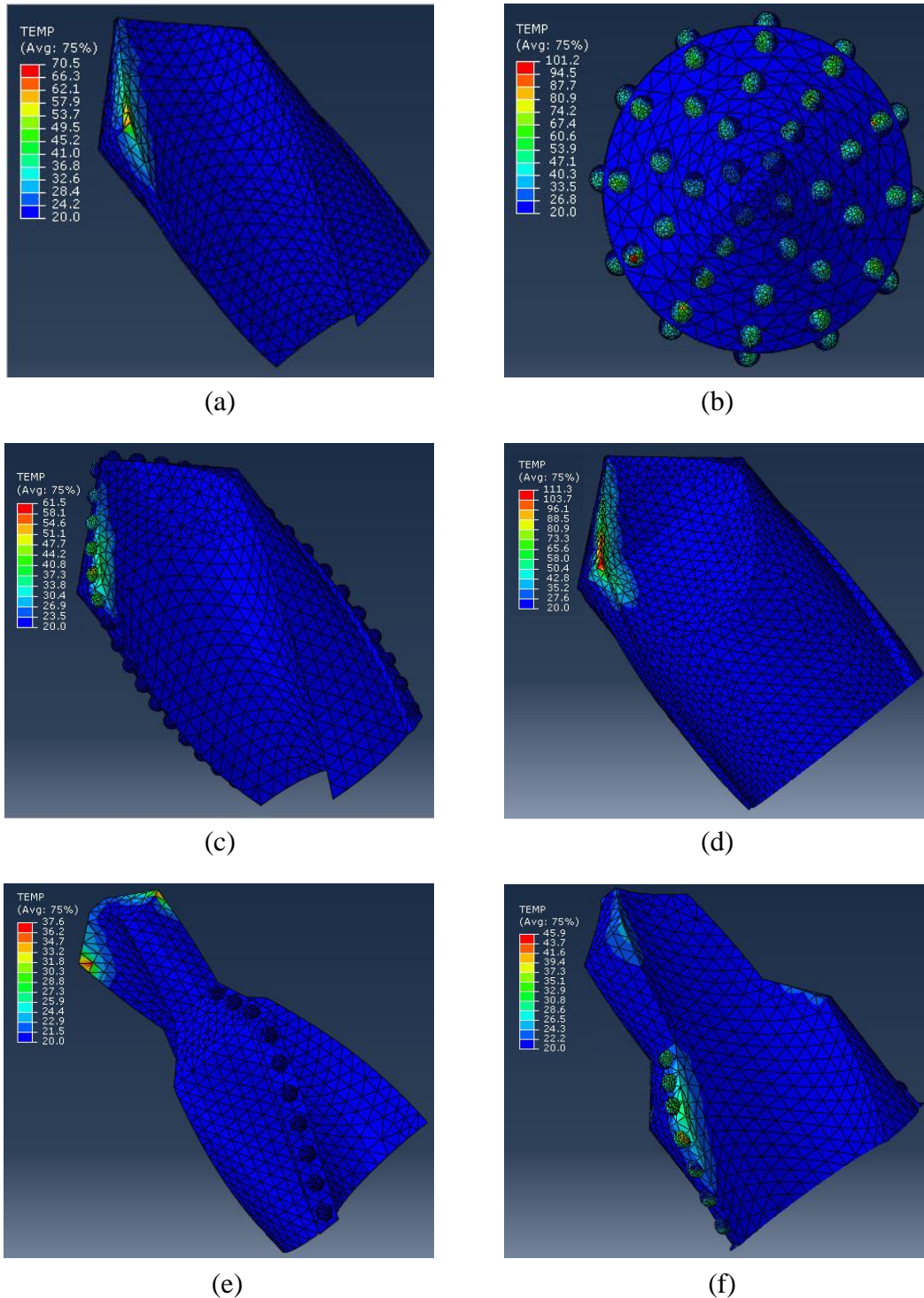


Fig. (10). Temperature distribution nephogram of different drills in steady state.

In Fig. (10a-f), obvious temperature gradient is seen at the drilling part. Color of the temperature gradient becomes shallow from the outer edge of main cutting edge to the chisel edge, indicating that the maximum temperature appears at the outer edge of main cutting edge.

The variation curves of maximum temperature of different drills against time are shown in Fig. (11 drill I, II, III, IV and V) represent brazed step drill, brazed twist drill, common twist drill, brazed abrasive drill and brazed PCBN superhard drill, respectively. As the drilling goes on, maximum temperatures of different drills all increase continuously. Combining Figs. (10 and 11), maximum temperatures of I, II, III, IV and V under steady state fluctuate at about 45.9°C, 61.5°C, 70.5°C, 101.2°C and 113.2°C, respectively. In Fig. (11), the maximum temperature curve of I have two equilibrium states. These are contributed by the drilling part and reaming part of the brazed step drill. The corresponding maximum temperatures read about 32.5°C and 45.9°C, respectively. Hence, drills with different structures show significantly different drilling temperatures. Brazed step drill shows the lowest drilling temperature, followed by brazed twist drill, standard twist drill, brazed abrasive drill and brazed PCBN superhard drill successively.

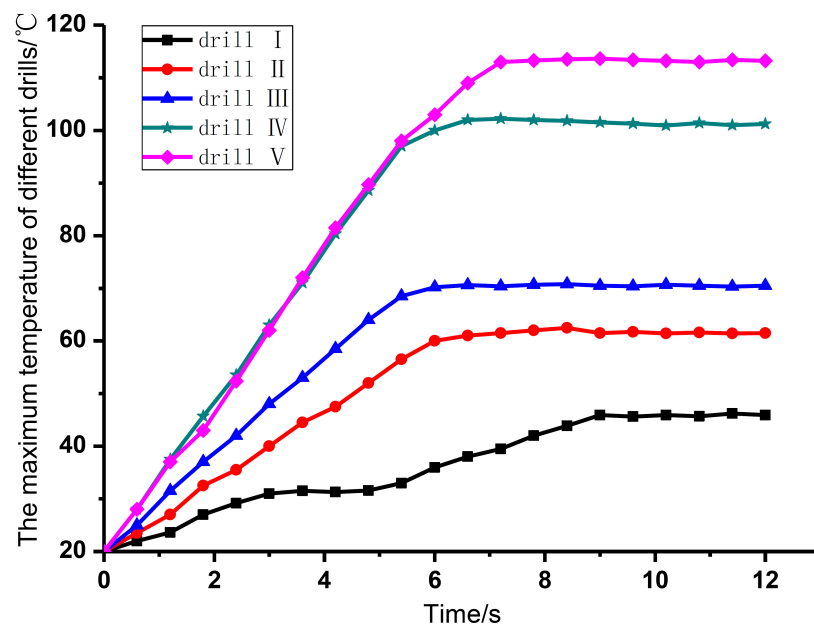


Fig. (11). The variation curves of maximum temperature of different drills against time.

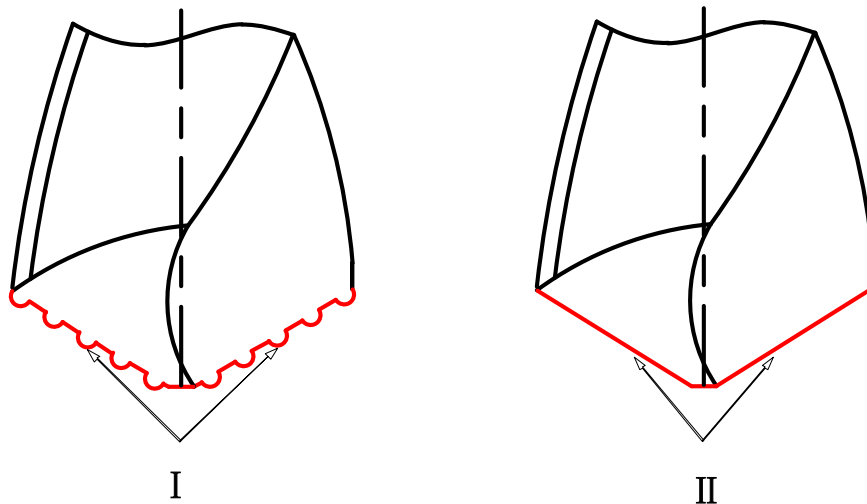
5. RESULTS AND DISCUSSION

Temperature fields on bone samples using five different drills were simulated. Simulation parameters include rotate speed $n=1000\text{rpm}$, feed speed $v_f=0.5\text{mm/s}$ and same properties of bone samples. Variation laws of the maximum temperature on drills and bone samples against time were concluded. Results showed that brazed step drill has the most ideal drilling temperature. It controls the maximum bone temperature below 47°C even under dry drilling. The maximum bone temperature of brazed twist drill is a little higher than 47°C. With appropriate cooling method, brazed twist drill also could provide ideal effect. On the contrary, drilling temperatures of common twist drill, brazed abrasive drill and brazed PCBN superhard drill increase successively. All of them are far higher than the critical temperature of osteonecrosis. To sum up, drill structure affects drilling temperature significantly.

Brazed step drill has the lowest drilling temperature and most ideal effect. This is mainly caused by smaller cutting material area per unit time under same drill diameter and drilling parameters, reducing heats generated by deformation and friction accordingly. During early drilling, brazed step drill could maintain same rotate speed and feed speed because of the small diameter of its drilling part, thus enabling to reduce cutting material area per unit time. During reaming process, the cutting material volume per unit time is also smaller than other drills since the middle drilling part has been cut. As a result, the drilling efficiency of brazed step drill declines, which gives cutting heats enough time to dissipate and avoids heat accumulation. In this way, drilling temperature decreases. On the other hand, the reaming part uses controllable orderly diamond abrasive particles for brazing rather than cutting edge in traditional twist drill. This is

similar with brazed twist drill, so that their temperature lowering mechanisms are basically same.

Compared to traditional twist drill, brazed twist drill has lower drilling temperature. This is mainly caused by the brazed controllable aligned diamond abrasive particles on the substrate of brazed twist drill. In the simulation model, diamond abrasive particles are simplified into spherical bodies. It can be seen clearly from Fig. (12) that the actual cutting edge of brazed twist drill involved in cutting is longer than that of common twist drill, but cutting material volume per unit time is fixed. Therefore, compared to common twist drill, brazed twist drill has larger cutting width and heat radiating area caused by drillings and the drill, but smaller cutting depth and deformation coefficient of drillings as well as fewer heats caused by plastic deformation. Combining heat yield and dissipation, brazed twist drill causes lower drilling temperature.



I-equivalent cutting edge of brazed twist drill; II- actual cutting edge of common twist drill

Fig. (12). Comparison between equivalent cutting edge of brazed twist drill and actual cutting edge of common twist drill.

Moreover, protrusion height of brazed diamond abrasive particles reaches as high as 70%~80%, which increases utilization of diamond and drill surface space for drillings significantly. When using traditional twist drill, drillings are extruded in the drill flute or between the drill and the workpiece, thus causing severe friction. In brazed twist drill, spaces between controllable aligned diamond abrasive particles could ensure drillings to pass through smoothly and avoids drillings block effectively, thus reducing drilling force and drilling temperature. On the other hand, diamond has strong thermal conductance and good heat dissipation. The thermal conductivity of diamond abrasive particle is as high as $2,200\text{w}/(\text{m}\cdot\text{K})$, while that of YG8 hard alloy is only $75.4\text{ w}/(\text{m}\cdot\text{K})$. This promises that generated drilling heats could dissipate through the drill as much as possible, thus lowering the drilling temperature. Additionally, diamond abrasive particles are characteristic of small friction coefficient and high hardness, which could reduce cutting force and frictional force during the drilling. This also could lower drilling temperature.

Brazed abrasive drill and brazed PCBN superhard drill cause sharp temperature rise during bone drilling. Although the diamond abrasive particles and PCBN superhard material have higher hardness, stronger thermal conductivity and smaller friction coefficient than other drill materials, brazed abrasive drill and brazed PCBN superhard drill are designed with no chip groove. Bone drillings may block abrasive particles or extrude between the drill and bone, increasing drilling force dramatically and generating abundant drilling heats which could be dissipated in time. Consequently, drilling temperature increases.

CONCLUSION

To overcome strong drilling force and over high temperature during orthopedic surgery, the four medical drills with different geometrical shapes by using superhard materials were designed. The bone drilling temperature field of superhard drill was theoretical analyzed. The following conclusions are drawn:

(1) Brazed step drill shows the lowest drilling temperature and controls it strictly below 47°C , the critical temperature of osteonecrosis. Brazed twist drill achieves the second lowest drilling temperature, a little higher than

47°C. Drilling temperatures of standard twist drill, brazed abrasive drill and brazed PCBN superhard drill increase successively. All of them exceed 47°C greatly.

(2) The maximum temperatures of brazed step drill, brazed twist drill, common twist drill, brazed abrasive drill and brazed PCBN superhard drill under steady state at about 45.9°C, 61.5°C, 70.5°C, 101.2°C and 113.2°C, respectively. Brazed step drill shows the lowest drilling temperature, followed by brazed twist drill, standard twist drill, brazed abrasive drill and brazed PCBN superhard drill successively.

CONFLICT OF INTEREST

The authors confirm that this article content has no conflict of interest.

ACKNOWLEDGEMENTS

This research was financially supported by the National Natural Science Foundation of China (51175276 and 51575290), Qingdao Science and Technology Program of Basic Research Projects (14-2-4-18-jch), and Huangdao District Application Science and Technology Project (2014-1-55).

REFERENCES

- [1] C. Pen, T. Xiao, and Y. Liang, "The changes of the methods and principles of the bone fracture treatments", *Med. Philos.*, vol. 26, no. 7, pp. 17-19, 2005.
- [2] G.X. Qi, and K.R. Dai, "Operative techniques in orthopaedic surgery", *Am. J. Chin. Med.*, vol. 17, no. 12, pp. 1283-1284, 2007.
- [3] Y.L. Hou, C.H. Li, H.L. Ma, Y.B. Zhang, M. Yang, and X.W. Zhang, "An experimental research on bone drilling temperature in orthopaedic surgery", *Open Mater. Sci. J.*, vol. 9, pp. 178-188, 2015.
[http://dx.doi.org/10.2174/1874088X01509010178]
- [4] A.B. Mullaji, T.L. Thomas, and M.S. Orth, "Low-energy subtrochanteric fractures in elderly patients: results of fixation with the sliding screw plate", *J. Trauma*, vol. 34, no. 1, pp. 56-61, 1993.
[http://dx.doi.org/10.1097/00005373-199301000-00010] [PMID: 8437196]
- [5] S.W. Wachtl, E. Gautier, and R.P. Jakob, "Low reoperation rate with the Medoff sliding plate: 1 technical failure in 63 trochanteric hip fractures", *Acta Orthop. Scand.*, vol. 72, no. 2, pp. 141-145, 2001.
[http://dx.doi.org/10.1080/000164701317323381] [PMID: 11372944]
- [6] R.A. Eriksson, T. Albrektsson, and B. Magnusson, "Assessment of bone viability after heat trauma. A histological, histochemical and vital microscopic study in the rabbit", *Scand. J. Plast. Reconstr. Surg.*, vol. 18, no. 3, pp. 261-268, 1984.
[http://dx.doi.org/10.3109/02844318409052849] [PMID: 6549359]
- [7] B.F. Guo, *Orthopaedic Surgery*. Scientific and Technological Documents Publishing Press: China, 2004.
- [8] G. Augustin, S. Davila, K. Mihoci, T. Udiljak, D.S. Vedrina, and A. Antabak, "Thermal osteonecrosis and bone drilling parameters revisited", *Arch. Orthop. Trauma Surg.*, vol. 128, no. 1, pp. 71-77, 2008.
[http://dx.doi.org/10.1007/s00402-007-0427-3] [PMID: 17762937]
- [9] S.R. Davidson, and D.F. James, "Drilling in bone: modeling heat generation and temperature distribution", *J. Biomech. Eng.*, vol. 125, no. 3, pp. 305-314, 2003.
[http://dx.doi.org/10.1115/1.1535190] [PMID: 12929234]
- [10] Y.X. Yang, C.Y. Wang, and Z. Qin, "Drilling force and temperature of bone by surgical drill", *Mach. Design Manuf.*, vol. 11, pp. 118-120, 2010.
- [11] T. Udiljak, D. Ciglar, and S. Skoric, "Investigation into bone drilling and thermal bone necrosis", *Adv. Prod. Eng. Manag.*, vol. 3, pp. 103-112, 2007.
- [12] L.S. Matthews, and C. Hirsch, "Temperatures measured in human cortical bone when drilling", *J. Bone Joint Surg. Am.*, vol. 54, no. 2, pp. 297-308, 1972.
[PMID: 4651263]
- [13] R.C. Vaughn, and F.A. Peyton, "The influence of rotational speed on temperature rise during cavity preparation", *J. Dent. Res.*, vol. 30, no. 5, pp. 737-744, 1951.
[http://dx.doi.org/10.1177/00220345510300051801] [PMID: 14888776]
- [14] J.R. Cameron, and J. Sorenson, "Measurement of bone mineral in vivo: an improved method", *Science*, vol. 142, no. 3589, pp. 230-232, 1963.
[http://dx.doi.org/10.1126/science.142.3589.230] [PMID: 14057368]
- [15] J.J. Sun, and J. Geng, "The mechanical properties of human cortical bone", *Adv. Mech.*, vol. 17, no. 2, pp. 200-215, 1987.
- [16] S. Karmani, "The thermal properties of bone and the effects of surgical intervention", *Curr. Orthop.*, vol. 20, no. 1, pp. 52-58, 2006.
[http://dx.doi.org/10.1016/j.cuor.2005.09.011]
- [17] M.T. Hillery, and I. Shuaib, "Temperature effects in the drilling of human and bovine bone", *J. Mater. Process. Technol.*, vol. 92, no. 9, pp.

- 302-308, 1999.
[[http://dx.doi.org/10.1016/S0924-0136\(99\)00155-7](http://dx.doi.org/10.1016/S0924-0136(99)00155-7)]
- [18] D. Knudson, *Fundamentals of Biomechanics*. Springer Press: Heidelberg, 2007.
- [19] Y.X. Yang, "Study on Drilling Performance of New Surgical Drill". Guangdong University of Technology, China, 2010.
- [20] H.L. Ma, and C.H. Li, *The axial force controllable surgical bone drill using abrasive drill*. China Patent ZL 201320016746.2, 2013.
- [21] H.L. Ma, and C.H. Li, *The axial force controllable surgical bone drill using brazed twist drill*. China Patent ZL 201320015561.X, 2013.
- [22] H.L. Ma, and C.H. Li, *The axial force controllable surgical bone drill using step drill*. China Patent ZL 201320020970.9, 2013.
- [23] H.L. Ma, and C.H. Li, *The axial force controllable surgical bone drill using brazed pcbn superhard material drill*. China Patent ZL201320016750.9, 2013.
- [24] G. Augustin, T. Zigman, S. Davila, T. Udiljak, T. Staroveski, D. Brezak, and S. Babic, "Cortical bone drilling and thermal osteonecrosis", *Clin. Biomech. (Bristol, Avon)*, vol. 27, no. 4, pp. 313-325, 2012.
[<http://dx.doi.org/10.1016/j.clinbiomech.2011.10.010>] [PMID: 22071428]
- [25] S.R. Davidson, and D.F. James, "Measurement of thermal conductivity of bovine cortical bone", *Med. Eng. Phys.*, vol. 22, no. 10, pp. 741-747, 2000.
[[http://dx.doi.org/10.1016/S1350-4533\(01\)00003-0](http://dx.doi.org/10.1016/S1350-4533(01)00003-0)] [PMID: 11334760]
- [26] S. Karmani, "The thermal properties of bone and the effects of surgical intervention", *Curr. Orthop.*, vol. 20, no. 1, pp. 52-58, 2006.
[<http://dx.doi.org/10.1016/j.cuor.2005.09.011>]
- [27] B.C. Sener, G. Dergin, B. Gursoy, E. Kelesoglu, and I. Slih, "Effects of irrigation temperature on heat control in vitro at different drilling depths", *Clin. Oral Implants Res.*, vol. 20, no. 3, pp. 294-298, 2009.
[<http://dx.doi.org/10.1111/j.1600-0501.2008.01643.x>] [PMID: 19397641]
- [28] G. Augustin, S. Davila, T. Udiljak, DS Vadrina, and D. Bagatin, "Determination of spatial distribution of increase in bone temperature during drilling by infrared thermography: preliminary report", *Arch. Orthop. Trauma Surg.*, vol. 129, no. 5, pp. 703-709, 2009.
- [29] J. Lee, O.B. Ozdoganlar, and Y. Rabin, "An experimental investigation on thermal exposure during bone drilling", *Med. Eng. Phys.*, vol. 34, no. 10, pp. 1510-1520, 2012.
[<http://dx.doi.org/10.1016/j.medengphy.2012.03.002>] [PMID: 22483188]
- [30] J. Lee, B.A. Gozen, and O.B. Ozdoganlar, "Modeling and experimentation of bone drilling forces", *J. Biomech.*, vol. 45, no. 6, pp. 1076-1083, 2012.
[<http://dx.doi.org/10.1016/j.jbiomech.2011.12.012>] [PMID: 22281407]
- [31] K. Alam, A.V. Mitrofanov, and V.V. Silberschmidt, "Experimental investigations of forces and torque in conventional and ultrasonically-assisted drilling of cortical bone", *Med. Eng. Phys.*, vol. 33, no. 2, pp. 234-239, 2011.
[<http://dx.doi.org/10.1016/j.medengphy.2010.10.003>] [PMID: 21044856]
- [32] Y.X. Yang, C.Y. Wang, and Z. Qin, "Drilling force and temperature of bone by surgical drill", *Adv. Mat. Res.*, vol. 126, pp. 779-784, 2010.
[<http://dx.doi.org/10.4028/www.scientific.net/AMR.126-128.779>]
- [33] R.K. Pandey, and S.S. Panda, "Drilling of bone: A comprehensive review", *J. Clin. Orthop. Trauma.*, vol. 4, no. 1, pp. 15-30, 2013.
[<http://dx.doi.org/10.1016/j.jcot.2013.01.002>] [PMID: 26403771]
- [34] N. Oliveira, F. Alaejos-Algarra, J. Mareque-Bueno, E. Ferrés-Padró, and F. Hernández-Alfaro, "Thermal changes and drill wear in bovine bone during implant site preparation. A comparative in vitro study: twisted stainless steel and ceramic drills", *Clin. Oral Implants Res.*, vol. 23, no. 8, pp. 963-969, 2012.
[<http://dx.doi.org/10.1111/j.1600-0501.2011.02248.x>] [PMID: 21806686]
- [35] M.C. Leeson, and S.B. Lippitt, "Thermal aspects of the use of polymethylmethacrylate in large metaphyseal defects in bone. A clinical review and laboratory study", *Clin. Orthop. Relat. Res.*, vol. 295, no. 295, pp. 239-245, 1993.
[PMID: 8403655]
- [36] M. Sumer, A.F. Misir, N.T. Telcioglu, A.U. Guler, and M. Yenisey, "Comparison of heat generation during implant drilling using stainless steel and ceramic drills", *J. Oral Maxillofac. Surg.*, vol. 69, no. 5, pp. 1350-1354, 2011.
[<http://dx.doi.org/10.1016/j.joms.2010.11.001>] [PMID: 21292371]
- [37] A. Marković, T. Mišić, B. Miličić, J.L. Calvo-Guirado, Z. Aleksić, and A. Đinić, "Heat generation during implant placement in low-density bone: effect of surgical technique, insertion torque and implant macro design", *Clin. Oral Implants Res.*, vol. 24, no. 7, pp. 798-805, 2013.
[<http://dx.doi.org/10.1111/j.1600-0501.2012.02460.x>] [PMID: 22469169]
- [38] N. Bertollo, H.R. Milne, L.P. Ellis, P.C. Stephens, R.M. Gillies, and W.R. Walsh, "A comparison of the thermal properties of 2- and 3-fluted drills and the effects on bone cell viability and screw pull-out strength in an ovine model", *Clin. Biomech. (Bristol, Avon)*, vol. 25, no. 6, pp. 613-617, 2010.
[<http://dx.doi.org/10.1016/j.clinbiomech.2010.02.007>] [PMID: 20359798]
- [39] J. Soriano, A. Garay, and P. Aristimuño, "Study and improvement of surgical drill bit geometry for implant site preparation", *Int. J. Adv. Manuf. Tech.*, vol. 74, no. 5-8, pp. 615-627, 2014.
[<http://dx.doi.org/10.1007/s00170-014-5998-x>]

- [40] S. Harder, C. Egert, H.J. Wenz, A. Jochens, and M. Kern, "Influence of the drill material and method of cooling on the development of intrabony temperature during preparation of the site of an implant", *Br. J. Oral Maxillofac. Surg.*, vol. 51, no. 1, pp. 74-78, 2013. [<http://dx.doi.org/10.1016/j.bjoms.2012.02.003>] [PMID: 22417718]
- [41] H.J. Oh, U.M. Wikesjö, H.S. Kang, Y. Ku, T.G. Eom, and K.T. Koo, "Effect of implant drill characteristics on heat generation in osteotomy sites: a pilot study", *Clin. Oral Implants Res.*, vol. 22, no. 7, pp. 722-726, 2011. [<http://dx.doi.org/10.1111/j.1600-0501.2010.02051.x>] [PMID: 21143537]
- [42] S. Sezek, B. Aksakal, and F. Karaca, "Influence of drill parameters on bone temperature and necrosis: a FEM modelling and in vitro experiments", *Comput. Mater. Sci.*, vol. 60, pp. 13-18, 2012. [<http://dx.doi.org/10.1016/j.commatsci.2012.03.012>]
- [43] F. Heinemann, I. Hasan, C. Kunert-Keil, W. Götz, T. Gedrange, A. Spassov, J. Schweppe, and T. Gredes, "Experimental and histological investigations of the bone using two different oscillating osteotomy techniques compared with conventional rotary osteotomy", *Ann. Anat.*, vol. 194, no. 2, pp. 165-170, 2012. [<http://dx.doi.org/10.1016/j.aanat.2011.10.005>] [PMID: 22056295]
- [44] V. Boner, P. Kuhn, T. Mendel, and A. Gisep, "Temperature evaluation during PMMA screw augmentation in osteoporotic bone--an in vitro study about the risk of thermal necrosis in human femoral heads", *J. Biomed. Mater. Res. B Appl. Biomater.*, vol. 90, no. 2, pp. 842-848, 2009. [<http://dx.doi.org/10.1002/jbm.b.31353>] [PMID: 19353575]
- [45] J.S. Nam, P.H. Lee, and S.W. Lee, "Experimental characterization of micro-drilling process using nanofluid minimum quantity lubrication", *Int. J. Mach. Tools Manuf.*, vol. 51, no. 7, pp. 649-652, 2011. [<http://dx.doi.org/10.1016/j.ijmactools.2011.04.005>]
- [46] K. Gok, A. Gok, and Y. Kisioglu, "Optimization of processing parameters of a developed new driller system for orthopedic surgery applications using Taguchi method", *Int. J. Adv. Manuf. Tech.*, vol. 76, no. 5-8, pp. 1437-1448, 2014.
- [47] C.H. Li, H.Y. Zhao, H.L. Ma, Y.L. Hou, Y.B. Zhang, M. Yang, and X.W. Zhang, "Simulation study on effect of cutting parameters and cooling mode on bone-drilling temperature field of superhard drill", *Int. J. Adv. Manuf. Technol.*, vol. 81, no. 9, pp. 2027-2038, 2015. [<http://dx.doi.org/10.1007/s00170-015-7259-z>]
- [48] L.D. Zhu, H.N. Li, and W.S. Wang, "Research on rotary surface topography by orthogonal turn-milling", *Int. J. Adv. Manuf. Technol.*, vol. 69, pp. 2279-2292, 2013.

© Hou *et al.*; Licensee Bentham Open.

This is an open access article licensed under the terms of the Creative Commons Attribution-Non-Commercial 4.0 International Public License (CC BY-NC 4.0) (<https://creativecommons.org/licenses/by-nc/4.0/legalcode>), which permits unrestricted, non-commercial use, distribution and reproduction in any medium, provided the work is properly cited.